Int. J. Electrochem. Sci., 6 **(2011)** 4341 - 4354

International Journal of
ELECTROCHEMICAL
SCIENCE
www.electrochemsci.org

Preparation of a Praseodymium Modified Ti/SnO_2-Sb/PbO_2 Electrode and its Application in the Anodic Degradation of the Azo Dye Acid Black 194

Zhiqiao He, Chengxiang Huang, Qiong Wang, Zhe Jiang, Jianmeng Chen, Shuang Song[*]

College of Biological and Environmental Engineering, Zhejiang University of Technology, Hangzhou 310032, People's Republic of China
[*]E-mail: ss@zjut.edu.cn

Received: 27 July 2011 / *Accepted:* 18 August 2011 / *Published:* 1 September 2011

A series of praseodymium modified Ti/SnO_2-Sb/PbO_2 (Ti/SnO_2-Sb/PbO_2-Pr) electrodes were synthesized by doping PbO_2 with praseodymium and the effect of Pr doping on the electrode catalytic activity toward the anodic oxidation of the model dye C.I. Acid Black 194 (AB-194) was examined in aqueous solution. The electrocatalytic activity of a Ti/SnO_2-Sb/PbO_2 electrode can be greatly improved by adding an appropriate amount of Pr into the PbO_2 layer. Accelerated life tests indicate that Pr doping also dramatically improves the stability of the Ti/SnO_2-Sb/PbO_2 anode. The introduction of Pr enhanced the formation of oxygen vacancies and surface hydroxyl groups, resulting in better activity and stability of the Ti/SnO_2-Sb/PbO_2-Pr electrode. A possible degradation pathway of AB-194 during the anodic oxidation process is proposed based on hydroxyl radical attack of the organic reactant.

Keywords: Ti/SnO_2-Sb/PbO_2 electrode; Praseodymium doping; Degradation; Activity and stability; Azo dye acid black 194

1. INTRODUCTION

It is estimated that approximately 800,000 t of dyes are manufactured annually worldwide, of which 50% are azo dyes. Azo dyes are typical environmental pollutants found in textile manufacturing [1]. Approximately 2-12% of dyes are lost during production and processing, and are then discharged into the water ecosystem as effluents [2], which can cause a severe environmental problem. Traditional treatments are inefficient for wastewater containing azo dyes due to the high chemical oxygen demand (COD), strong color, large amount of suspended solids, variable pH, as well as salt content and the

high temperatures required [3, 4]. For these reasons advanced electrochemical oxidation processes for the degradation of dye-polluted wastewater have attracted considerable attention due to having three major advantages: high energy efficiency, a fast reaction rate and easy operation when compared with other conventional processes [5-9]. Furthermore, electrochemical oxidation processes consume fewer chemicals and produce no sludge. On the other hand, electrochemical oxidation processes are commonly performed at room temperature and atmospheric pressure, thus reducing the possibility of volatilization and discharge of untreated residues [10, 11].

Although anodic oxidation processes are a potentially superior technique for the treatment of wastewater, the lack of suitable anodes is still a major problem. Many studies have revealed that the complete destruction of organic compounds can be performed efficiently by anodic oxidation processes using high oxygen overvoltage anodes, such as RuO_2, PbO_2 and boron-doped diamond (BDD) [12-14]. Among them, the PbO_2 electrode has received considerable attention due to its high electrical conductivity, high oxygen evolution potential, chemical inertness and low cost [15-18].

Metal cations have been shown to vary the catalytic activity and oxygen atom transfer properties of the PbO_2 [19, 20]. Various metals have been incorporated into PbO_2 by co-electrodeposition to form doped PbO_2 electrodes, such as Ce-PbO_2 [21], Bi- PbO_2 [22], Co-PbO_2 [23] and Fe-PbO_2 [24]. Previous studies have demonstrated that the catalytic activity and stability of the PbO_2 electrode can be increased significantly by doping using these metal oxides.

Praseodymium ions can exchange between trivalent and tetravalent states, thereby allowing the release and uptake of oxygen [25, 26]. We suggest that praseodymium could be a potentially useful candidate dopant for chemical modified electrodes. There are also few previously reported studies on the Pr modified PbO_2 electrode (Ti/SnO_2-Sb/PbO_2-Pr).

Herein, the dye C.I. Acid Black 194 (AB-194, CAS No.61931-02-0) was chosen as a representative dye to explore the application of electrochemical oxidation on Ti/SnO_2-Sb/PbO_2-Pr electrodes for the efficient removal of azo dyes in aqueous solution. The effects of different doping levels on the COD reduction were evaluated, and the accelerated life was tested. Furthermore, a mechanism of AB-194 anodic oxidation is proposed by measuring levels of the intermediates during the reaction process.

2. EXPERIMENTAL

2.1. Materials and chemicals

AB-194 was obtained from Zhejiang Xincheng Co., Ltd., Shaoxing, China and was used without further purification. Praseodymium nitrate ($Pr(NO)_3$•$6H_2O$) was purchased from Aladdin Reagent Co., Ltd., Hangzhou, China. All other chemicals, including acetone, ethanol, butanol, HCl, $SnCl_4$, Sb_2O_3, HNO_3, $Pb(NO_3)_2$, NaF, NaOH, H_2SO_4, and NaCl were of analytical grade quality and bought from Huadong Medicine Co., Ltd., Hangzhou, China. All solutions were prepared with doubly distilled water.

2.2. Electrode preparation and characterization

The detailed procedure for the preparation of the Ti/SnO_2–Sb/PbO_2 electrode has been previously described in the literature [27-29]. To prepare for a good adhesive metal oxide film, the titanium substrate was pretreated according to the following procedures before anodization: Firstly, titanium sheets (99.5%, 20 mm × 30 mm) were degreased in absolute ethanol for 20 min by sonic oscillation, polished on 320-grit paper strips, and then cleaned with water; secondly, the sheets were etched in boiling aqueous 20% hydrochloric acid for 1 h; finally, they were washed copiously with doubly distilled water. The titanium plates were now gray and had lost their metallic sheen.

The SnO_2-Sb coating, which was to be deposited onto the pretreated titanium substrate, was prepared by electrodeposition of the inner coating layer and thermal deposition of the outer layer. This was then used as a substrate for the electrodeposition of undoped and Pr-doped PbO_2 films to improve the performance of Ti/SnO_2-Sb/PbO_2 and Ti/SnO_2-Sb/PbO_2-Pr electrodes.

The undoped PbO_2 film was electrodeposited at 65 ^oC in a 0.07 M HNO_3 solution containing 0.5 M Pb^{2+}, added as $Pb(NO_3)_2$, and 0.04 M NaF for 20 min. The current was maintained at 80 mA cm^{-2} and the voltage was ~3.5 V. The preparation of PbO_2-Pr films was as previously described, except for the addition of $Pr(NO_3)_3$•$6H_2O$ to the electrolyte. The electrodes with ratios of praseodymium atoms to lead atoms in electrodeposition solutions of 1:100, 1:20, and 1:10 are denoted as Ti/SnO_2-Sb/PbO_2-1%Pr, Ti/SnO_2-Sb/PbO_2-5%Pr and Ti/SnO_2-Sb/PbO_2-10%Pr, respectively.

Generally, the prepared electrode has a three-layer structure: an inner layer of Ti substrate, an intermediate layer of electrochemical and thermally deposited SnO_2-Sb, and an outer active layer of electrodeposited PbO_2 or PbO_2-Pr.

X-ray diffraction (XRD) patterns were gathered using a Thermo ARL SCINTAG X'TRA X-ray diffraction meter, with Cu Kα radiation in the range of 10–80°. Surface images came from a Philips XL-30 scanning electron microscopy (SEM) for analyzing the topography of prepared films.

After dissolving in concentrated hydrochloric acid, the amount of Pr on the electrode was accurately measured using a Perkin Elmer ELAN DRC-e inductively coupled plasma mass spectrometer (ICP-MS). It was measured that the Pr content was 0.58, 1.35 and 2.28 g m^{-2} for Ti/SnO_2-Sb/PbO_2-1%Pr, Ti/SnO_2-Sb/PbO_2-5%Pr and Ti/SnO_2-Sb/PbO_2-10%Pr electrodes, respectively.

2.3. Electrochemical experiments

The electrolysis of aqueous solutions containing the dye were carried out in a two-compartment electrochemical system [30], with anodes of either Ti/SnO_2-Sb/PbO_2 or Ti/SnO_2-Sb/PbO_2-Pr electrodes (20 mm × 30 mm) and platinum sheet (20 mm × 30 mm) as a cathode. The prepared working electrode was placed in 160 mL of the aqueous dye anolyte with 0.1 M Na_2SO_4 as the supporting electrolyte, and the catholyte was 60 mL aqueous solution containing 0.1 M Na_2SO_4. A Nafion-117 membrane was used as a cation exchange membrane to separate the anolyte from the catholyte. The electrode gap between the anode and cathode was ~80 mm. During each run, the electrolyte was maintained at 25 ± 3 ^oC and stirred using a magnetic follower to enhance mass transfer. Samples were collected from the anodic compartment at preset intervals and were taken for chemical

analysis. A constant current (30 mA cm^{-2}) between the counter electrode and the working electrode was determined with a multimeter.

The cyclic voltammetry (CV) measurements were carried out at room temperature utilizing a conventional three-electrode system with a computer-controlled CHI 660C electrochemical workstation. The laboratory-made Ti/SnO_2-Sb/PbO_2 and Ti/SnO_2-Sb/PbO_2-Pr anodes were used as working electrodes, a platinum sheet (20 mm × 30 mm) and a saturated Ag/AgCl electrode were used as the counter and reference-electrode, respectively.

The accelerated life test was conducted according to the procedure described by Zhou et al. [9]. Typically, we kept the anodic current density at a constant of 1200 mA cm^{-2} in a 9 M H_2SO_4 electrolyte at 90 ± 0.5 ^oC. The potential of the working electrodes was monitored periodically and the operational time at which the potential increased by 5 V above the initial value was considered as the accelerated life of the electrode.

2.4. Analytical method

COD was measured based on standard methods for the examination of water and wastewater [31]. The current efficiency (CE), representing the ratio of the current effectively used in the electrooxidation of organics at a given time to the applied current, was calculated using the following relation [32]:

$$\mathrm{CE}(\%)=\frac{\mathrm{COD}_t-\mathrm{COD}_{t+\Delta t}}{8I\Delta t}FV\times 100$$

Where COD_t and $COD_{t+\Delta t}$ are the COD (mg L^{-1}) at times t and $t+\Delta t$ (s), respectively; F is the Faraday constant (96487 C mol^{-1}), V is the volume of the electrolyte (L), I is the current (A), and 8 is the equivalent mass of oxygen (g mol^{-1}).

A Varian cp 3800 gas chromatograph with a Varian Saturn 2000 mass spectrometer (GC-MS) was used to identify the organic intermediates. A wall coated open tubular (WCOT) fused silica series column (30 m × 0.25 mm, 0.25 μm film thickness) was used and the temperature held at 60 ^oC for 2 min, then increased at a rate of 8 ^oC min^{-1} to 150 ^oC, and then held at that temperature for 5 min. The temperature was then increased to 220 ^oC at a rate of 8 ^oC min^{-1} and held for 5 min. Electron impact (EI) ionization was done at 70 eV, using the carrier gas helium, with injection temperature of 250 ^oC and injection flow was set at 0.8 mL min^{-1}.

3. RESULTS AND DISCUSSION

3.1. Electrode characterization

XRD can be used to determine the crystalline structure and lattice parameters of a material. The wide-angle XRD analyses of the Ti/SnO_2-Sb/PbO_2 and Ti/SnO_2-Sb/PbO_2-Pr electrodes with various Pr contents are shown in Fig. 1.

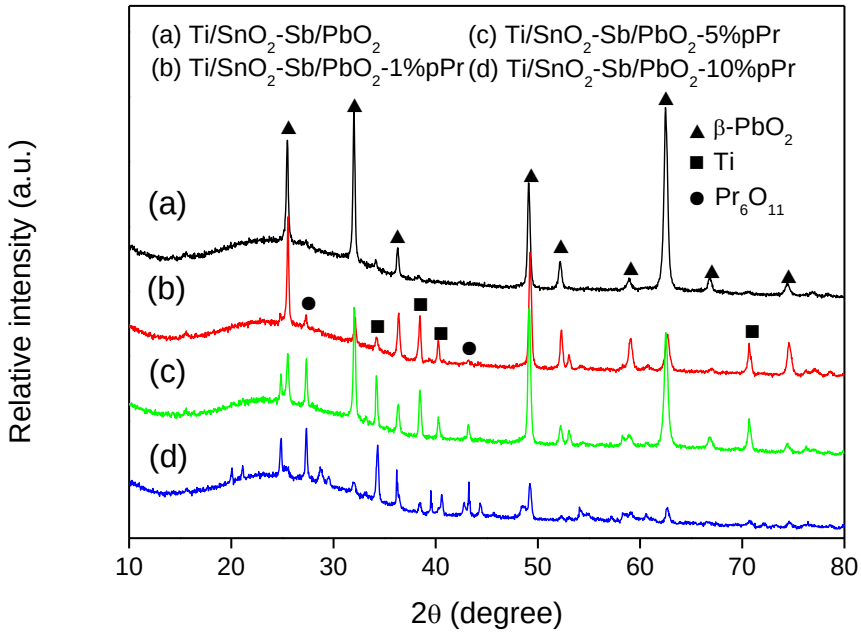

Figure 1. The XRD patterns of Ti/SnO_2-Sb/PbO_2 (a), Ti/SnO_2-Sb/PbO_2-1%Pr (b), Ti/SnO_2-Sb/PbO_2-5%Pr (c) and Ti/SnO_2-Sb/PbO_2-10%Pr electrodes (d).

All the samples clearly show the diffraction from the (110), (101), (200), (211), (220), (310), (301), (202), (321) planes of β-PbO_2, with respect to the 2θ values, having values of approximately 25.5°, 32.0°, 36.3°, 49.1°, 52.1°, 59.0°, 62.5°, 66.8° and 74.4°, respectively. Also, the planes of the Pr_6O_{11} at 2θ values of 27.3° and 43.2° appear on the Pr doped electrodes. Similar to Ce doping onto PbO_2 film, the formation of praseodymium oxide in PbO_2 crystals may be caused by the electrooxidation of Pr cations being chemically adsorbed on the growing oxide deposit of PbO_2. The existence of other new phases was not observed with Pr doping, indicating that the β-PbO_2 phase was not thoroughly changed in our experiments. Also, the relative intensities of the (100), (002), (101), (103) planes of the Ti substrate were enhanced with increasing Pr amount, suggesting that the surface of the Ti/SnO_2-Sb/PbO_2-Pr electrodes were more porous and rough. This was further confirmed by the SEM results.

In addition, we found that the relative intensities of the (110), (101), (301) peaks of PbO_2 were attenuated with increasing Pr content, showing that the praseodymium oxides may provide a new center for PbO_2 to nucleate, which inhibits the growth of PbO_2 crystals [33, 34]. Furthermore, the diffraction pattern at 2θ values of approximately 27.3° was markedly enlarged. This result can be ascribed to typical reflection of the (111) planes of Pr_6O_{11}.

To further check the impact of Pr doping on the formation of PbO_2, the electrode crystal structure and appearance were observed using SEM. Fig. 2 shows the morphologies of Ti/SnO_2-Sb/PbO_2 and Ti/SnO_2-Sb/PbO_2-Pr electrodes with a magnification of 3000 times. It is obvious from the mass contrast that all the electrodes have pyramid-shaped morphologies. In image a, the surface of the Ti/SnO_2-Sb/PbO_2 electrode is almost uniform and the PbO_2 particle size is evaluated to be micronsized. In images b, c and d, the electrode surfaces are rough and many “cracks” could be

observed. Also, the particle sizes appear relatively larger in cases where more Pr was introduced into the deposition solution.

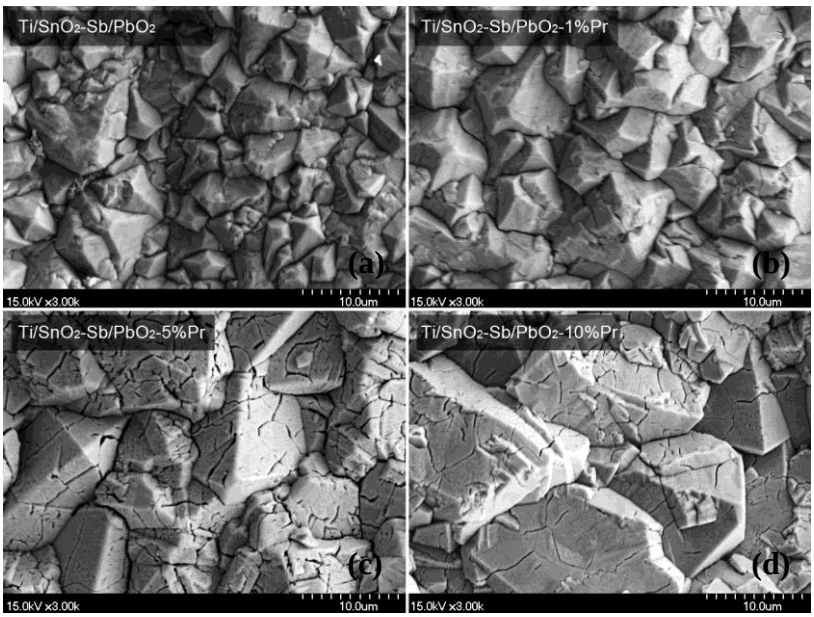

Figure 2. The SEM images of Ti/SnO_2-Sb/PbO_2 (a), Ti/SnO_2-Sb/PbO_2-1%Pr (b), Ti/SnO_2-Sb/PbO_2-5%Pr (c) and Ti/SnO_2-Sb/PbO_2-10%Pr electrodes (d).

The aforementioned outcome can be attributed to Pr_6O_{11} formation, changing the nucleation and growth of crystals in the films. Pr_6O_{11} can be regarded as the complex compound with 4 PrO_2 and Pr_2O_3 [35]. The ionic radius of Pr^{4+} is 90 pm, which is very close to that of Pb^{4+} (84 pm). From the view of radius matching, it is possible for quadrivalent praseodymium to form a solid solution with lead oxide via substitution during the process of electrodeposition [36, 37]. Meanwhile, the corresponding Pr^{3+} ions have a larger ionic radius (101 pm) and therefore could be responsible for expansion of surface particles.

3.2. Cyclic voltammetry

CV measurements were used to investigate the electrochemical performance of the electrodes upon the electrochemical degradation of AB-194. Fig. 3 displays the cyclic voltammograms for the Ti/SnO_2-Sb/PbO_2 and Ti/SnO_2-Sb/PbO_2-5%Pr electrodes in a 0.1 M Na_2SO_4 electrolyte solution containing 100 mg L^{-1} AB-194 at a scan rate of 100 mV s^{-1}. The blank curve was given as a basis for comparison of the measured results with and without Pr doping under the same experimental conditions.

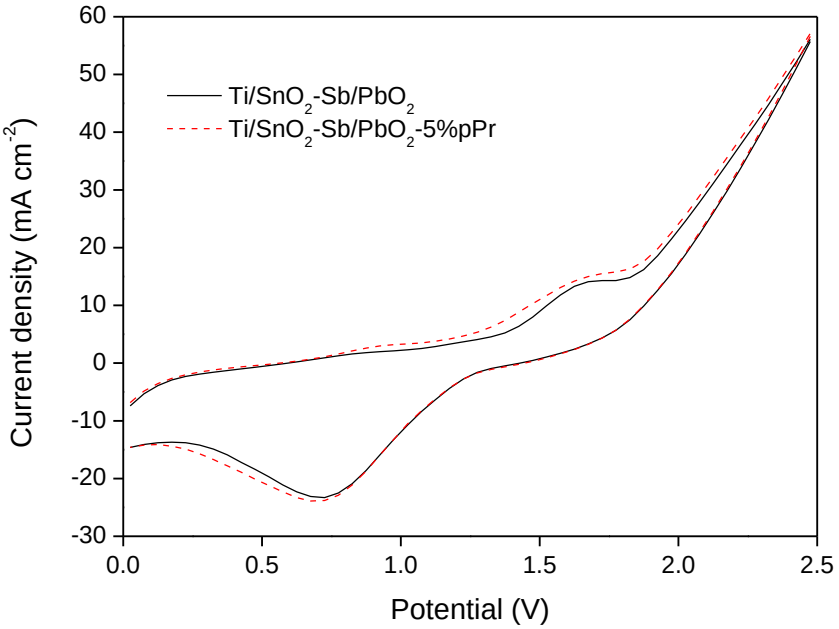

Figure 3. The CVs of Ti/SnO_2-Sb/PbO_2 and Ti/SnO_2-Sb/PbO_2-5%Pr anode in the presence of AB-194: scan rate, 100 mV s^{-1}; initial concentration of AB-194, 100 mg L^{-1}; concentration of supporting electrolyte (Na_2SO_4), 0.1 M.

Anodic current peaks at ~1.50 V and cathodic current peaks at ~0.70 V were observed for both electrodes, representing the oxidation and reduction of Pb(IV)/Pb(II)/Pb(0) couples, as validated by other researchers [38, 39]. No additional peak can be found from these CV curves, suggesting that the dye degradation occurs exclusively via indirect electrochemical oxidation, which is mediated by •OH radicals, rather than direct electron transfer. Furthermore, similar CV curves are also observed on the Pr-doped electrode except the currents are at a slightly higher value than those of the undoped electrode. This could be possibly attributed to the better electro-conductivity of the Ti/SnO_2-Sb/PbO_2-5%Pr electrode.

3.3. Enhanced electrode activities

The COD reduction is the determining factor which reflects the electrochemical capabilities of the different electrodes, such as the capabilities of direct electron transfer and radical production, in the oxidation of parent substances and any intermediate species produced. Hence, the COD reduction efficiency during anodic oxidation was studied to examine the correlation between electrochemical activity and doped-Pr content.

Fig. 4 depicts the results of electrochemical degradation of AB-194 and the corresponding CE among the electrodes with various Pr contents after 10 h of electrolysis. The Ti/SnO_2-Sb/PbO_2-Pr electrodes reveal substantially enhanced activity for the degradation of AB-194 compared to the Ti/SnO_2-Sb/PbO_2 electrode.

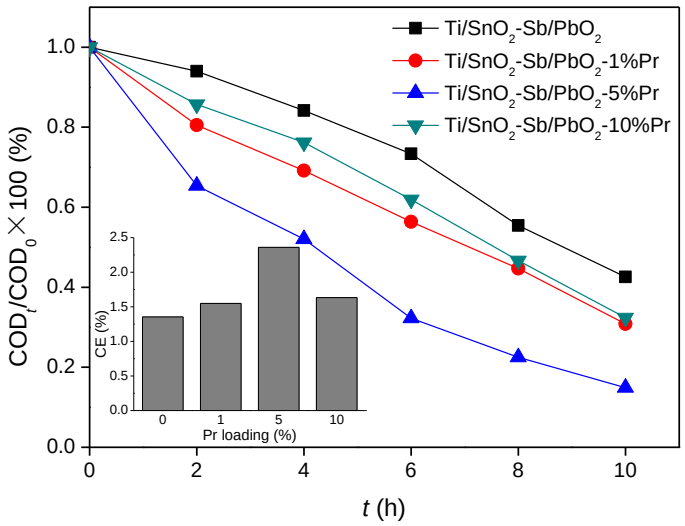

Figure 4. Influence of Pr loading on the degradation of AB-194 (the inset is the CE after 10 h reaction): initial concentration of AB-194, 100 mg L^{-1}; current density, 30 mA cm^{-2}; concentration of supporting electrolyte (Na_2SO_4), 0.1 M.

The electrochemical activity of the Ti/SnO_2-Sb/PbO_2-Pr electrode increases with increasing Pr content up to 5% (the optimum metal doping level) and then decreased. The COD removal using the Ti/SnO_2-Sb/PbO_2-5%Pr electrode was more than 1.5 times greater compared to the undoped one. The CE exhibits a similar trend with a maximum value of ~2.3% in the range studied. It appears that Pr doping of a Ti/SnO_2-Sb/PbO_2 electrode results in a superior electrocatalytic degradation of the dye AB-194.

The PbO_2 anode is generally considered to be a non-active electrode [40]. It is well accepted that •OH radicals are firstly electro-generated by water discharge.

$$PbO_2 + H_2O \rightarrow PbO_2(\bullet OH) + H^+ + e^- \quad (1)$$

Then the hydroxyl radicals can be electrochemically oxidized to oxygen.

$$PbO_2(\bullet OH) \rightarrow PbO_2 + \frac{1}{2}O_2 + H^+ + e^- \quad (2)$$

Or alternatively can assist oxidation of the organic compound to CO_2 and H_2O, as the hydroxyl radicals are weakly adsorbed on PbO_2 surface.

$$PbO_2(\bullet OH) + \text{organics} \rightarrow PbO_2 + mCO_2 + nH_2O + H^+ + e^- \quad (3)$$

It has been previously reported that the generation of •OH radicals is dependant on the structure of the PbO_2 electrode. The formation of the •OH radical is proposed to be localized in a certain number of 'active centers' [41]. Like Ce doping, Pr might afford more active sites for reaction (1), consequently promoting the anodic oxidation of AB-194 [34]. In addition, it is suggested that the catalytic activity of the anode could be improved with a higher number of oxygen vacancies, which in turn increases the conductivity of the PbO_2 film [42].

It is believed that the concentration of surface hydroxyl groups is proportional to the number of oxygen vacancies in aqueous solution [43]. To confirm whether the concentration of oxygen vacancies was varied with Pr doping, the surface hydroxyl group on the electrode was determined by reference to the literature [44, 45]. Table 1 shows that the concentration of surface hydroxyl groups are increased with an increased Pr content in the Ti/SnO_2-Sb/PbO_2-Pr electrode, implying the increase of more oxygen vacancies. This can be explained by the fact that Pr_6O_{11} can be considered as an oxygen deficient modification of a cubic fluorite-like PrO_2 structure [46], which exhibits a high oxygen mobility. Thus, the electrocatalytic ability of the Ti/SnO_2-Sb/PbO_2 electrode was greatly enhanced after doping with praseodymium by means of increasing the number of oxygen vacancies.

However, as previously stated, the electrocatalytic ability of a Ti/SnO_2-Sb/PbO_2-Pr electrode decreased with 10% doping level of Pr. The poor performance of the Ti/SnO_2-Sb/PbO_2-10%Pr electrode may be due to the limitation of Pr atoms to incorporate into the PbO_2 lattice. Excessive addition of Pr would lead to the Pr deposition on the surface of PbO_2 film, reducing the electrocatalytic performance.

3.4. Improved electrode stability

Stability is another important factor that governs the application of an electrode. It is difficult to evaluate the actual lifetimes of electrodes in different applications, because lifetimes are deeply influenced by working conditions such as current density, pH and the temperature of the electrolyte. In this study, both the undoped and the Ti/SnO_2-Sb/PbO_2-5%Pr electrodes were subjected to accelerated life tests to compare their electrode stability. Table 1 shows that the Ti/SnO_2-Sb/PbO_2 electrode is estimated to have a service life of ~96 h. Close observation of the surface of the electrode, conductive oxide film and the titanium substrate showed corrosion and part of the titanium substrate was dissolved into the solution. In comparison, to the modified one, the Ti/SnO_2-Sb/PbO_2-5%Pr electrode displayed excellent stability up to ~424 h, much longer than that of the Ti/SnO_2-Sb/PbO_2 electrode under analogous conditions.

The mechanism which results in electrode deactivation appears complex, including metal base passivation, film consumption, film detachment, and mechanical damage [47]. One of the most important factors responsible for electrode stability is the bonding quality between the film and substrate. The tensile stresses between the PbO_2 coating and Ti substrate are beneficial to ensure the electrode stability, whereas compressive and interfacial stresses are the main causes of film detachment [48]. During the process of an accelerated life test, the partial active oxygen atoms

produced gradually occupy the oxygen vacancies and oxide the Ti substrate, which results in the transition of intrinsic stresses from tensile to compressive and interfacial.

Table 1. Physicochemical parameters of the prepared electrodes.

Samples	Actual Pr content (g m^{-2})	Crystal phase composition	Morphology	Number of surface OH groups (mmol m^{-2})	CE (%) after 10 h electrolysis	Accelerated life (h)
Ti/SnO_2-Sb/PbO_2	0	β-PbO_2	uniform pyramid-shape	77.7	1.35	~96
Ti/SnO_2-Sb/PbO_2-1%Pr	0.58	β-PbO_2, Pr_6O_{11}	rough pyramid-shape	129.4	1.55	—
Ti/SnO_2-Sb/PbO_2-5%Pr	1.35	β-PbO_2, Pr_6O_{11}	rough pyramid-shape	155.4	2.36	~424
Ti/SnO_2-Sb/PbO_2-10%Pr	2.28	β-PbO_2, Pr_6O_{11}	rough pyramid-shape	166.5	1.63	—

Subsequently, the PbO_2 anodes rapidly become inactive due to the peeling away of the active layer [48, 49]. Therefore, we can conclude that the existence of oxygen vacancies facilitate the maintenance of electrode stability. As previously discussed, compared with a Ti/SnO_2-Sb/PbO_2 electrode, there are more oxygen vacancies in the Ti/SnO_2-Sb/PbO_2-Pr electrode, which induces more tensile stresses. Accordingly, the lifetime of a Ti/SnO_2-Sb/PbO_2 electrode has been greatly prolonged after modification by praseodymium.

Hine et al. have proposed an empirical relationship between the electrode service life (SL) and the current density (*i*) [50], which can be used to assess the actual life of a Ti/SnO_2-Sb/PbO_2-5%Pr electrode for use in different applications;

$$SL \sim \frac{1}{i^n} \qquad 4$$

where *n* ranges from 1.4 to 2.0. Assuming an average *n* value of 1.7 for the electrode, the service life of Ti/SnO_2-Sb/PbO_2-5%Pr was predicted to be 3.9 years in application under current density of 100 mA cm^{-2}.

3.5. A possible degradation mechanism

Determination of the major intermediates formed during the electrocatalytic process is helpful in obtaining further insight into the reaction mechanism. The intermediates produced during the electrochemical degradation of AB-194 were detected by GC-MS and the results are given in Table 2. The technique of acidification was used prior to GC-MS analysis. No sulfur isotopic peak was identified for any sample analyzed. This demonstrates there are no S-containing organic materials in the samples studied, and that sulfonic moieties were removed rapidly from AB-194 by anodic oxidation.

On the basis of the GC-MS findings; a possible degradation pathway for the AB-194 anodic oxidation is illustrated by Fig. 5. Cleavage of the bonds C(4)–N and C(11)–N seem to occur first by

free hydroxyl radical attack on the dye molecule, which led to the decolorzing of AB-194 in the bulk solution.

Table 2. Intermediates of AB-194 degradation identified by GC-MS

Symbol	Compound	Structural formula	Sample time (h)						
			0.5	1	2	4	6	8	10
D1	6-nitronaphthalene-1,2-diol	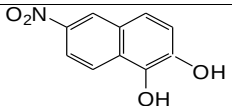	√	×	×	×	×	×	×
D2	1,2-naphthalenediol	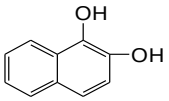	√	√	×	×	×	×	×
D3	phthalic acid	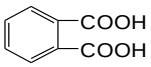	√	√	√	√	×	×	×
D4	benzoic acid	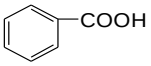	×	√	√	√	×	×	×
D5	maleic acid		×	×	√	√	√	√	√
D6	oxalic acid		×	×	√	√	√	√	√
D7	acrylic acid	CH_2=CHCOOH	×	×	√	√	√	√	√

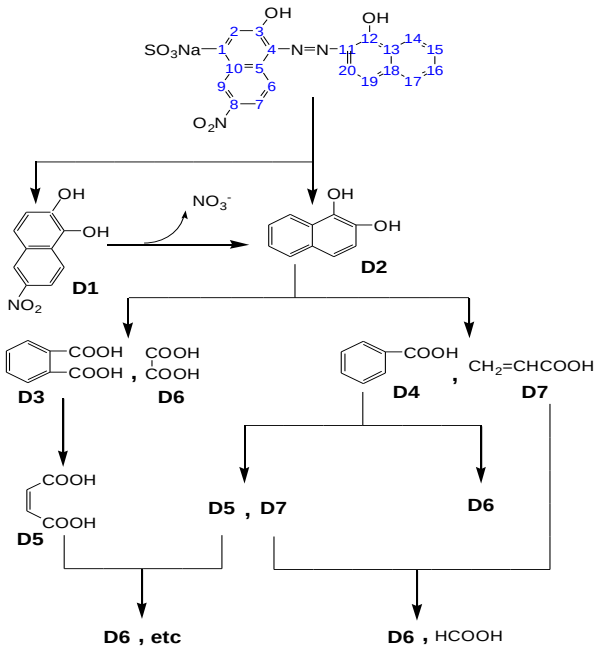

Figure 5. Probable degradation pathway of electrochemical oxidation of AB-194 on Ti/SnO_2-Sb/PbO_2-5%Pr anode: initial concentration of AB-194, 100 mg L^{-1}; current density, 30 mA cm^{-2}; concentration of supporting electrolyte(Na_2SO_4), 0.1 M.

Earlier studies suggest that the azo group has decomposed due to the elimination of molecular nitrogen [51]. This proposal was supported by the fact that 6-nitronaphthalene-1,2-diol (**D1**) and 1,2-naphthalenediol (**D2**) were detected in a sample collected at 0.5 h. Additionally, compound **D1** can be further oxidized to yield compound **D2** by denitration. Subsequently, compound **D2** might be converted into phthalic acid (**D3**) or benzoic acid (**D4**), via cleavage of the benzene ring by oxidation with active •OH radicals. This is accompanied by the generation of some small molecules such as oxalic acid (**D6**) and acrylic acid (**D7**). Under the electrooxidation conditions, the compounds **D3** and **D4** would be further transformed into maleic acid (**D5**) and the compound **D7**, which would finally be converted into some small molecule acid such as compound **D6** and formic acid, etc. Alternatively, compound **D4** may also be directly converted to compound **D6** through a ring cleavage process.

4. CONCLUSIONS

This work is an investigation of the improvement of Ti/SnO_2-Sb/PbO_2 anodes when doped with praseodymium, and their application in the electrocatalytic degradation of the azo dye AB-194. The active layers of the Ti/SnO_2-Sb/PbO_2 and Ti/SnO_2-Sb/PbO_2-Pr electrodes were prepared by an electrodeposition method. The results of XRD and SEM techniques show that diffraction peaks corresponding to Pr_6O_{11} could be found and the surface of Ti/SnO_2-Sb/PbO_2 electrode, which became cracked and rougher after Pr modification, indicating the Pr cationic species can be incorporated into PbO_2 by co-electrodeposition to form Ti/SnO_2-Sb/PbO_2-Pr electrodes.

The electrochemical degradation of AB-194 using the Ti/SnO_2-Sb/PbO_2-Pr anodes was faster than that of using an undoped one under analogous conditions. Among them, the Ti/SnO_2-Sb/PbO_2-5%Pr anode exhibits the best performance. Additionally, the accelerated life test implied that the Ti/SnO_2-Sb/PbO_2-Pr electrode had favorable electrochemical stability. More yields of oxygen vacancies and surface hydroxyl groups are thought to be responsible for the enhancement of activities and stabilities of Ti/SnO_2-Sb/PbO_2 anodes caused by praseodymium doping.

Overall, the Ti/SnO_2-Sb/PbO_2-Pr electrode seems to be a promising alternative anode for the treatment of wastewater which contains organic pollutants due to a high electrocatalytic activity and an enhanced service life.

ACKNOWLEDGEMENTS

This work was supported by the National Natural Science Foundation of China (Grant Nos. 20977086 and 21076196), National Basic Research Program of China (Grant No. 2009CB421603), and Zhejiang Provincial Natural Science Foundation of China (Grant Nos. Z5080207 and Y5100310).

References

1. H. Zollinger, Color Chemistry: Synthesis, Properties and Applications of Organic Dyes and Pigments, 2nd ed., V.C.H. Publisher, New York, 1991.
2. C.A. Martinez-Huitle and E. Brillas, *Appl. Catal. B: Environ.*, 87 (2009) 105.

3. S.H. Lin and C.F. Peng, *Water Res*., 28 (1994) 277.
4. S.H. Lin and C.F. Peng, *Water Res*., 30 (1996) 587.
5. Y.L. Hsiao and K. Nobe, *J. Appl. Electrochem*., 23 (1993) 943.
6. K. Rajeshwar, J.G. Ibanez and G.M. Swain, *J. Appl. Electrochem*., 24 (1994) 1077.
7. Y.M. Awad and N.S. Abuzaid, *Sep. Sci. Technol*., 34 (1999) 699.
8. C. Comninellisa, *Electrochim. Acta*, 39 (1994) 1857.
9. M.H. Zhou, Q.Z. Dai, L.C. Lei, C.A. Ma and D.H. Wang, *Environ. Sci. Technol*., 39 (2005) 363.
10. L.S. Andrade, T.T. Tasso, D.L. Da Silva, R.C. Rocha, N. Bocchi and S.R. Biaggio, *Electrochim. Acta*, 54 (2009) 2024.
11. J. Parkes, *J. Cleaner Prod*., 2 (1994) 83.
12. C. Comninellis and C. Pulgarin, *J. Appl. Electrochem*., 23 (1993) 108.
13. A.M. Polcaro, S. Palmas, F. Renoldi and M. Mascia, *J. Appl. Electrochem*., 29 (1999) 147.
14. M. Panizza and G. Cerisola, *Ind. Eng. Chem. Res*., 47 (2008) 6816.
15. M.A. Quiroz, S. Reyna, C.A. Martinez-Huitle, S. Ferro and A.De Battisti, *Appl. Catal. B: Environ*., 59 (2005) 259.
16. M. Panizza and G. Cerisola, *Appl. Catal. B: Environ*., 75 (2007) 95.
17. D.C. Johnson, J. Feng and L.L. Houk, *Electrochim. Acta*, 46 (2000) 323 .
18. M.H. Zhou, Z.C. Wu, X.J. Ma, Y.Q. Cong, Q. Ye and D.H. Wang, *Sep. Purif. Technol*., 34 (2004) 81.
19. N.D. Popovic, J.A. Cox and D.C. Johnson, *J. Electroanal. Chem*., 456 (1998) 203.
20. N.B. Tahar and A. Savall, *J. Appl. Electrochem*., 29 (1999) 277.
21. Y.H. Song, G. Wei and R.C. Xiong, *Electrochim. Acta*, 52 (2007) 7022.
22. Y. Liu, H.L. Liu, J. Ma and X. Wang, *Appl. Catal. B: Environ*., 91 (2009) 284.
23. L.S. Andrade, R.C. Rocha-Filho, N. Bocchi, S.R. Biaggio, J. Iniesta, V. Garcia-García and V. Montiel, *J. Hazard. Mater*., 153 (2008) 252.
24. L.S. Andrade, L.A.M. Ruotolo, R.C. Rocha, N. Bocchi, S.R. Biaggio, J. Iniesta, V. Garcia-García and V. Montiel, *Chemosphere*, 66 (2007) 2035.
25. Z.Q. He, A.L. Zhang, S. Song, Z.W. Liu, J.M. Chen, X.H. Xu and W.P. Liu, *Ind. Eng. Chem. Res*., 49 (2010) 12345.
26. P. Sonstrom, J. Birkenstock, Y. Borchert, L. Schilinsky, P. Behrend, K. Gries, K. Muller, A. Rosenauer and M. Baumer, *ChemCatChem*, 2 (2010) 694.
27. S. Song, L.Y. Zhan, Z.Q. He, L.L. Lin, J.J. Tu, Z.H. Zhang, J.M. Chen and L.J. Xu, *J. Hazard. Mater*., 175 (2010) 614.
28. X.Y. Li, Y.H. Cui, Y.J. Feng, Z.M. Xie and J.D. Gu, *Water Res*., 39 (2005) 1972.
29. Y.J. Feng and X.Y. Li, *Water Res*., 37 (2003) 2399.
30. S. Song, J.Q. Fan, Z.Q. He, L.Y. Zhan, Z.W. Liu, J.M. Chen and X.H. Xu, *Electrochim. Acta*, 55 (2010) 3606.
31. APHA, AWWA, WPCF, Standard Methods for the Examination of Water and Wastewater, American Public Health Association, Washington, DC, USA, 1998.
32. C. Comninellis and C. Pulgarin, *J. Appl. Electrochem*., 21 (1991) 703.
33. J.T. Kong, S.Y. Shi, L.C. Kong, X.P. Zhu and J.R. Ni, *Electrochim. Acta*, 53 (2007) 2048.
34. Y. Liu, H.L. Liu, J. Ma and J.J. Li, *Electrochim. Acta*, 56 (2011) 1352.
35. M. Chen, K.L. Huang, X.A. Mei, C.Q. Huang, J. Liu and A.H. Cai, *Trans. Nonferrous Met. Soc. China*, 19 (2009) 138.
36. G. Liu, Z.G. Chen, C.L. Dong, Y.N. Zhao, F. Li, G.Q. Lu and H.M. Cheng, *J. Phys. Chem. B*, 110 (2006) 20823.
37. L.G. Devi and S.G. Kumar, *Appl. Surf. Sci*., 257 (2011) 2779.
38. A.Czerwinski and M. Zelazowska, *J. Power Sources*, 64 (1997) 29.
39. A.Czerwinski, M. Zelazowska, M. Grden, K. Kuc, J.D. Milewski, A. Nowacki, G. Wojcik and M. Kopczyk, *J. Power Sources*, 85 (2000) 49.

40. C. Comninellis, *Electrochim. Acta*, 39 (1994) 1857.
41. D. Pavlov and B. Monahov, *J. Electrochem. Soc*., 143 (1996) 3616.
42. S. Abaci, K. Pekmez and A. Yildiz, *Electrochem. Commun*., 7 (2005) 328.
43. S. Song, Z.W. Liu, Z.Q. He, A.L. Zhang and J.M. Chen, *Environ. Sci. Technol*., 44 (2010) 3913.
44. E. Laiti, L. Ohman, J. Nordin and S. Sjoberg, *J. Colloid Interface Sci*., 175 (1995) 230.
45. H. Tamura, A. Tanaka, K. Mita and R. Furuichi, *J. Colloid Interface Sci*., 209 (1999) 225.
46. G.A.M. Hussein, *J. Anal. Appl. Pyrolysis*, 37 (1996) 111.
47. G.N. Martelli, R. Ornelas and G. Faita, *Electrochem. Acta*, 39 (1994) 1551.
48. J.L. Cao, Z.C. Wu, H.X. Li and J.Q. Zhang, *Acta Phys. -Chim. Sin*., 23 (2007) 1515.
49. W. Buckel, *J. Vac. Sci. Technol*., 6 (1969) 606.
50. F. Hine, M. Yasuda, T. Noda, T. Yoshida and J. Okuda, *J. Electrochem. Soc*., 126 (1979) 1439.
51. F. Gahr, F. Hermanutz and W. Oppermann, *Water Sci. Technol*., 30 (1994) 255.

© 2011 by ESG (www.electrochemsci.org)